TUNGSTEN CONTROL IN NBI-DOMINANT H-MODE DISCHARGES IN EAST TOKAMAK

L. Zhang[1]
[1]Institute of Plasma Physics Chinese Academy of Sciences, Hefei 230026, Anhui, China
Email: zhangling@ipp.ac.cn

S. Morita[2,3], X. D. Yang[4], Z. Xu[5,6], X. Z. Gong[1], M. H. Li[1], Y. M. Duan[1], Y. Y. Li[1], Y. W. Sun[1], J. Huang[1], F. Ding[1], L. Wang[1], Y. Liu[1], Q. Zang[1], H. Q. Liu[1], G. S. Xu[1], Z. W. Wu[1], H. Y. Guo[7], C. D. Hu[1], J. L. Chen[1], L. Q. Hu[1], Y. F. Liang[1,8], X. D. Zhang[1] and EAST Team

[2]National Institute for Fusion Science, Toki 509-5292, Gifu, Japan
[3]Graduate University for Advanced Studies, Toki 509-5292, Gifu, Japan
[4]Science Island Branch of Graduate School, University of Science and Technology of China, Hefei 230026, China
[5]Advanced Energy Research Center, Shenzhen University, Shenzhen 518060, China
[6]Key Laboratory of Optoelectronic Devices and Systems of Ministry of Education and Guangdong Province, College of Optoelectronic Engineering, Shenzhen University, Shenzhen 518060, China
[7]General Atomics, San Diego, California 92186, USA
[8]Association EURATOM-FZJ, Trilateral Euregio Cluster, D-52425 Jülich, Germany

Abstract

In EAST tokamak, H-mode discharges have been obtained at various heating conditions despite the installation of tungsten monoblocks at upper divertor. Recently, a reproducible long pulse H-mode operation with sufficient tungsten suppression has succeeded for both electron cyclotron resonance (ECR) and lower-hybrid wave (LHW) heated discharges, and various experimental approaches are also attempted for the tungsten suppression. In discharges dominantly heated by neutral beam injection (NBI), however, the long pulse H-mode operation has been often restricted by appearance of the tungsten accumulation. In order to control the tungsten accumulation in the NBI H-mode discharges, experiments have been done by superimposing the LHW heating. Since plasma particles are pumped out after switching on the LHW pulse, the tungsten concentration is largely reduced in the plasma core, while the tungsten emission in the plasma outer region is also reduced. In addition, radial profiles of line emissions from highly ionized tungsten ions and radiation measured with AXUV and soft x-ray arrays show that the tungsten distribution is considerably flattened during the LHW pulse, although the tungsten ions accumulate in a very narrow region of core plasmas ($\rho<0.2$) during the NBI phase. The results clearly indicate effects of the LHW on edge screening and core transport of tungsten ions in the NBI H-mode discharge. When the power ratio of P_{LHW}/P_{NBI} is relatively high, e.g. ~0.9, the tungsten concentration is sufficiently reduced by an order of magnitude. A beneficial role on the LHW injection to control the tungsten concentration in the NBI discharge is observed for the first time in EAST suggesting a potential way toward steady-state H-mode NBI operation.

1. INTRODUCTION

In recent magnetic confinement fusion research high-Z material of tungsten is one of important plasma facing materials (PFMs) due to the good characteristics of high sputtering threshold, small retention of tritium and high neutron resistance. The tungsten is used for ITER divertor material instead of carbon [1], and is also planned for CFETR divertor [2]. In order to examine an effect of the tungsten divertor on the tokamak discharge, several tokamak devices have installed the tungsten as a plasma facing component (PFC), e.g. ASDEX-U [3] and WEST [4] with full tungsten environment, JET with ITER-like wall [5] and EAST with tungsten monoblock upper divertor [6]. EAST tokamak has been also equipped with upper tungsten divertor since 2014 to improve the heat exhaust capability and to examine the ITER-like divertor configuration [6].

In EAST tokamak, H-mode discharges have been obtained at various heating conditions despite the installation of tungsten monoblocks at upper divertor. Recently, a reproducible long pulse H-mode operation with sufficient tungsten suppression has succeeded for both ECH and LHW heated discharges, and various experimental approaches are also attempted for the tungsten suppression [7]. In discharges with relatively high power NBI, however, the long pulse H-mode operation has been often restricted by appearance of the tungsten

accumulation. In EAST, therefore, an experimental scenario capable of avoiding the tungsten accumulation is energetically explored for achieving the long pulse H-mode NBI discharge with high-performance plasmas. Until now it is reported from ASDEX-U and JET [8-10] that on-axis ECRH and ICRH can be applied to suppress the tungsten accumulation. In the present report, a beneficial role of the LHW injection on the tungsten accumulation suppression observed for the first time in EAST is presented.

2. EXPERIMENTAL SETUP

EAST is a full superconducting tokamak device with flexible divertor configuration, i.e. lower single null, double null and upper single null configurations. After equipment of ITER-like W/Cu monoblock in upper divertor, EAST has been routinely operated at upper single null configuration with high injection power to access steady-state discharges with high performance plasmas. Recently, several heating systems have been upgraded in EAST. It enables to explore multiple heating schemes on the H-mode discharge study. In this work, the heating systems applied to the H-mode discharge study are co- and counter-injection NBIs ($P_{co\text{-}NBI}$=$P_{ctr\text{-}NBI}$=4MW, $E_{co\text{-}NBI}$= $E_{ctr\text{-}NBI}$=50-80keV) [11], two ECR (f_{ECRH}=140GHz, P_{ECRH}=1.0MW) [12] and LHW [13] (f_{LHW}=4.6GHz, P_{LHW}=6MW). The LHW frequency of 4.6GHz is used at a parallel refractive index of $n_{//}$ = 2.04 and a phase difference between adjacent main waveguides of 90° to achieve the best coupling efficiency.

To study the tungsten behavior in EAST H-mode discharges, tungsten spectra have been measured by a fast-time-response EUV spectrometer with time resolution of 5ms working in wavelength ranges of 20-500Å (EUV_Long) [14]. In addition a space-resolved EUV spectrometer working in 30-520Å (EUV_Long2) [15] has been used to measure the radial profile of line emissions from highly ionized tungsten ions in H-mode discharges. The tungsten concentration, C_W, is evaluated with a combination of intensities of the tungsten unresolved transition array (W-UTA) in 45-70Å and total radiation loss [16]. In the experiment radial profiles of electron temperature, T_e, are provided by Thomson scattering diagnostic [17] and 16-channel heterodyne radiometer [18], radial profiles of electron density, n_e, are measured by polarimeter-intferometer [19] and microwave reflectometry [20]. Tungsten source from upper divertor is evaluated from line intensity of W I at 4009 Å measured by divertor visible spectroscopy [21]. Radiation power loss is evaluated from extreme ultraviolet (AXUV) signals [22].

3. RADIATION COLLAPS DUE TO TUNGSTEN ACCUMULATION

In earlier EAST experiments, it was found that the tungsten easily accumulated in the plasma core in NBI H-mode discharges when the ELM frequency, f_{ELM}, was low, e.g. 20-30Hz [23]. Typical results on the tungsten concentration, C_W, in NBI discharges are shown in Fig. 1. When the NBI power increases from 0.8 to 3.0MW, the value of C_W increases from 4.0×10^{-6} to 3.0×10^{-4}, as illustrated in Fig. 1. H-L back transition or plasma disruption often occurs when the NBI power is high. It is noted that the ELM frequency is relatively high, e.g. f_{ELM}~100-200Hz. Therefore, the H-mode operational widow against plasma current, I_p, in NBI H-mode discharges is strictly limited to I_p~0.4MA because the tungsten accumulation always occurs at high I_p, i.e. $I_p\geq$0.6MA.

Recently, discharges with the multiple heating scheme are attempted to control the tungsten accumulation, e.g. LHW and ECRH superposed on NBI discharges. However, the tungsten concentration is increased by two order of magnitude, when the injected RF power, P_{LHW}+P_{ECRH}, is not sufficient, e.g., P_{LHW}+$P_{ECRH}\leq$1.5MW. Fig. 2 illustrates a typical NBI-dominant discharge (shot #62965, I_p=0.6MA, B_t=2.25T, P_{NBI}=2.8MW, P_{LHW}=1.7MW) with tungsten accumulation in EAST. After the second NBI is superposed on the first NBI at t=3.5s, L-H transition appears, followed by an ELM-free H-mode phase. However, the radiation power gradually increases with the density increase, indicating that the tungsten accumulation occurs. At the same moment the discharge performance starts to deteriorate toward the plasma collapse which is occurred within 0.5s from the second NBI injection. On the other hand, a smooth discharge is sometimes disturbed by a tungsten dust arising from upper tungsten divertor. The dust behavior is always monitored with fast visible cameras in EAST. The tungsten dust seems to originate in a certain leading edge of the upper tungsten divertor plate. A drastical increase in the tungsten concentration and radiation power is observed after the appearance of tungsten dust. Even if the tungsten dust is relatively small, it easily causes the H-L back transition. The value of C_W is analyzed at the H-L

back transition and plasma disruption. The results are also shown in Fig. 1 with solid triangle and square. It is clear that the threshold of Cw ranges in $6.0\times10^{-5} \le C_W \le 3.0\times10^{-4}$.

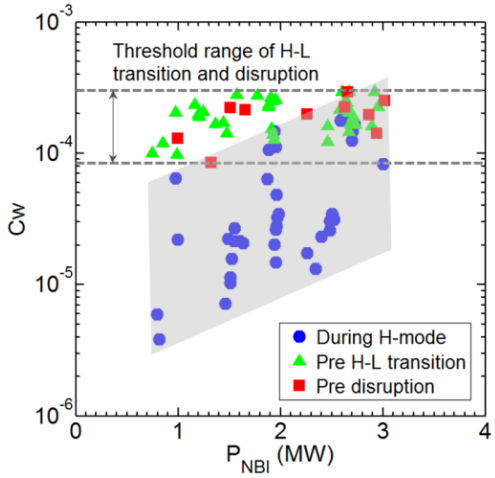

Fig. 1. Tungsten concentration in core plasma, C_W, as a function of NBI power during ELMy H-mode phase (solid blue circles), H-L transition (solid green triangles) and plasma disruption (solid red squares) in NBI H-mode discharges. Two dashed lines indicate the threshold range of C_W to H-L back transition and disruption.

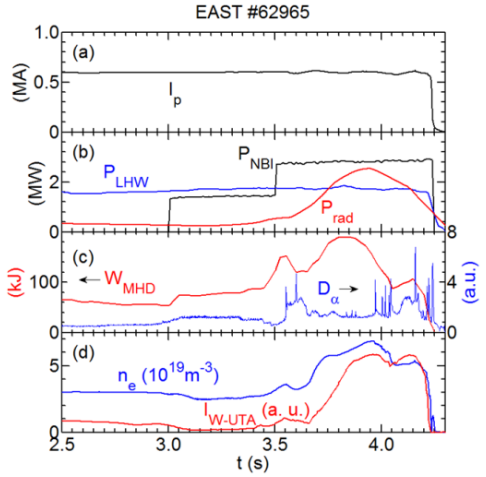

Fig. 2. Typical example of plasma collapse due to tungsten accumulation. Time evolutions of (a) plasma current, Ip, (b) LHW power, P_{LHW}, NBI power, P_{NBI}, and total radiation power loss, P_{rad}, (c) plasma store energy, W_{MHD}, and upper divertor D_α, and (d) line-averaged electron density, n_e, and intensity of tungsten UTA in shot #62965.

Since the tungsten source could not be experimentally identified with divertor visible spectroscopy system by measuring the WI (400.9nm) line in the tungsten dust event, the intensity of edge AXUV signal at ρ~0.9 is used by normalizing the intensity by the electron density as the edge tungsten flux. The Cw shown in Fig. 1 is replotted in Fig. 3 as function of the edge tungsten flux.

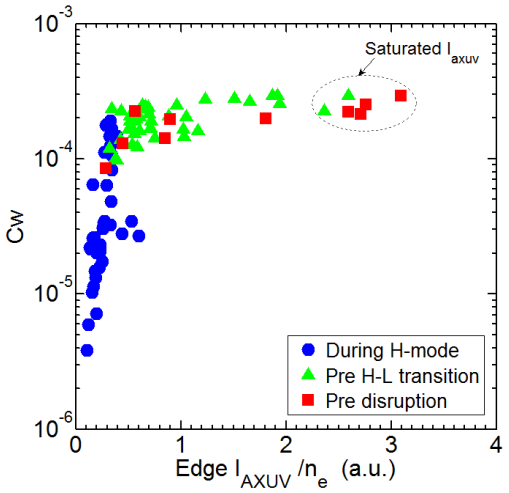

Fig. 3. Tungsten concentration in core plasmas, C_W, as function of edge AXUV radiation at ρ~0.9 normalized by electron density

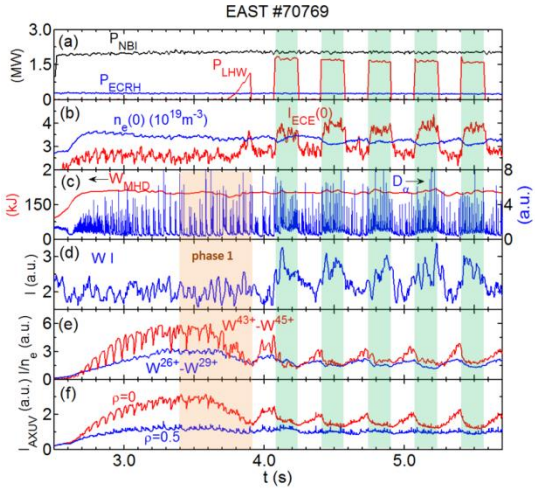

Fig. 4. Time evolutions of (a) P_{NBI}, P_{ECRH} and P_{LHW}, (b) $n_e(0)$ and $I_{ECE}(0)$, (c) W_{MHD} and divertor D_α, (d) W^{43+} - W^{45+} intensity at plasma core and W^{26+} - W^{29+} intensity at plasma outer region and (e) $P_{rad}(0)$ and $P_{rad}(0.5)$. Timings of LHW injection are indicated with shaded area

4. TUNGSTEN SUPPRESSION WITH INJECTION OF LHW

In recent EAST experiments, real-time lithium powder injection has been caried out in H-mode discharges to suppress the tungsten source [24]. However, the tungsten still exists in the core plasma with considerable high concentration. In order to control the tungsten accumulation in NBI H-mode discharges, experiments have been also done by superimposing the LHW heating. Initial result on the tungsten suppression is obtained in H-mode discharges at P_{LHW}>>P_{NBI} [23]. For a comprehensive understanding on the combined heating of LHW and NBI and further better control of the tungsten accumulation, several heating combinations have been explored in EAST.

One of the experiments is carried out by intermittently changing the 4.6GHz LHW power during the NBI H-mode phase. Figure 4 illustrates a typical result on the intermittent injection of the LHW. The LHW with P_{LHW}=1.5MW is injected during a steady phase of the NBI discharge with P_{NBI}=2.0MW with frequency of 3Hz and duty cycle of 50%. Low-power ECH with P_{ECRH}=0.3MW is also injected during the whole discharge period to sustain the electron temperature. Before the LHW pulse is switched on, an improvement of the particle confinement after the L-H transition is clearly seen in the temporal density behavior at t=2.6s. Reflecting the particle confinement improvement, the tungsten content continuously increases during 2.6-3.2s.

When the LHW pulse is switched on, the electron density shown in Fig. 4(b) starts to decrease, suggesting the particle pump out. At the same time the f_{ELM} starts to increase and reached 80Hz, while the f_{ELM} decreases to 60-70Hz after the LHW pulse. The ELM amplitude also starts to increase and keeps the high level until the end of LHW pulse (see Fig. 4(c)). During the LHW pulse the tungsten source from WI line emission is continuously increased by 50-80% (see Fig. 4(d)). However, the tungsten concentration in the plasma outer region slightly decreases. It can be suggested by temporal behaviors of line emissions from W^{26+}-W^{29+} (W^{26+} at 49.0Å, W^{27+} at 49.4 Å and W^{29+} 49.8 Å in Fig. 6(b)) normalized by n_e (see Fig. 4(e)). Further interest is seen in the temporal behavior of core tungsten emissions from W^{43+}-W^{45+} ions (W^{45+} at 62.336Å, W^{44+} at 60.93 Å and W^{43+} 61.334 Å in Fig. 6(b)) normalized by n_e plotted in Fig. 4(e)). It indicates the tungsten concentration in the plasma core largely decreases during the LHW phase, while it continuously increases during the NBI phase.

Similar big change is also observed in the central chord (ρ=0) of the radiation loss shown in Fig. 4(f). When the LHW pulse is switched off, the tungsten concentration returns to the original level before the LHW is switched on. The radial profiles of T_e and n_e are shown in Figs 5 (a) and (b) as function of normalized minor radius, ρ, respectively. The data are taken at t=4.85s during the LHW pulse and at t=5.0s between the two LHW pulses in the discharge shown in Fig. 4. The profiles do not change so much between two cases with and without LHW. It means the big change in the tungsten emissions does not originate in changes of the temperature and density profiles.

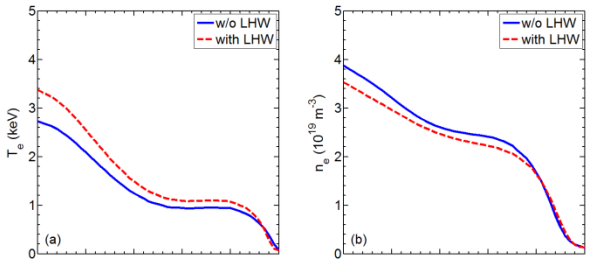

Fig. 5. Comparison of radial profiles of (a) electron temperature, T_e, and (b) electron density, n_e, during the H-mode phase with and without 4.6GHz LHW injection in shot #70769.

Typical tungsten spectra observed during the LHW pulse and before the LHW pulse in shot #70769 are shown in the Fig. 6(b). As a comparison typical tungsten spectra observed in other two discharges with lower T_e (I_p=0.4MA, P_{NBI}=2.5MW, P_{LHW}=1.0 and 2.0MW, $T_e(0)\leq$2.0keV) are also shown in Fig. 6(a). It is understood that in the low T_e discharges only the W-UTA spectra composed of lower ionization stages are observed, while in the shot #70769 with high T_e many emission lines from highly ionized tungsten ions, i.e. W^{40+}-W^{45+}, are observed with strong intensity not only in the W-UTA spectra at 45-70Å but also in longer wavelength range of 120-140 Å as isolated lines. The intensity of such tungsten lines is obviously reduced with increasing the injected LHW power for both low and high T_e H-mode discharges. The spectra analyzed here also indicates results on the tungsten suppression.

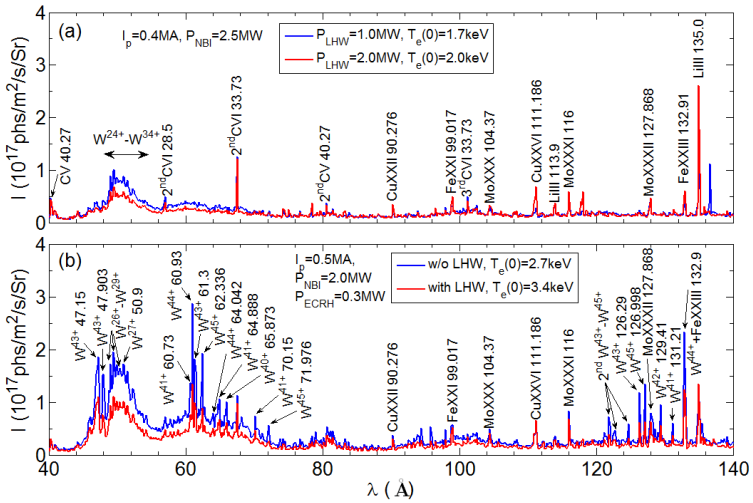

Fig. 6 Typical tungten spectra in wavelength range of 40-140Å during (a) two NBI H-mode discharges with different injection LHW power of 1MW and 2MW, and (b) two phases with and without LHW pulse in NBI H-mode discharges at shot #70769.

The radial profile of tungsten line intensities is observed with a space-revolved EUV spectrometer. In NBI discharges the CCD is routinely operated in full image (FI) mode to identify a pixel with big noise caused by high-energy neutral particles. Then, a longer cycle time of 800ms is necessary for the sufficient exposure time. Figure 7 illustrates vertical intensity profiles of line emissions from W^{45+} (62.336Å), W^{44+} (60.93 Å), W^{43+} (61.334 Å) and W^{27+} (50.9 Å) during the NBI phase at t=3.2-4.0s in Fig. 4 and during the LHW phase. It is found that the vertical intensity profiles from W^{43+}-W^{45+} ions are strongly peaked during the NBI phase. However, the profiles are flattened during the LHW phase with extremely low intensity. Even in the W^{27+} line located at outer plasma region the intensity is clearly reduced during the LHW phase (see Fig. 7(d)). These profile data also indicates an effective suppression of the tungsten ions from core plasmas in NBI discharges with LHW.

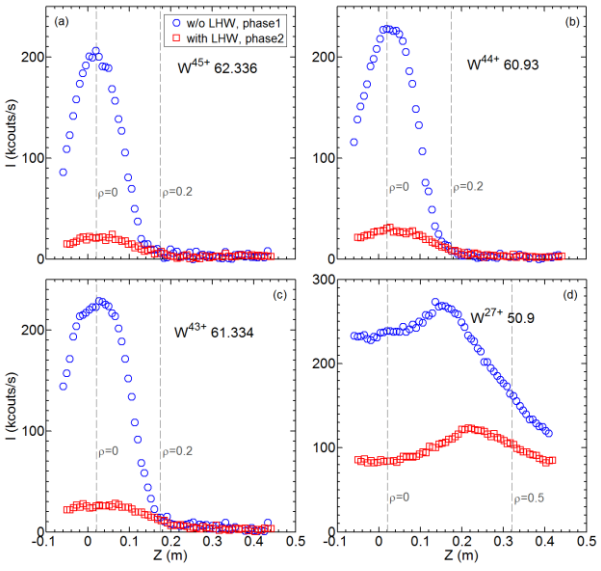

Fig. 7 Vertical intensity profile of (a) W^{45+} (62.336Å), (b) W^{44+} (60.93Å), (c) W^{43+} (61.334 Å) and (d) W^{27+} (50.9 Å) in W-UTA spectra during H-mode phase without LHW (phase1 in shot #70769) and steady-state H-mode phase with LHW (shot #79746). The radial locations of ρ=0, 0.2 and 0.5 are indicated with vertical dash lines.

Time behaviors of radial radiation distributions measured with AXUV array from shot #70769 are shown in Figs. 8. The result indicates that the tungsten accumulates in a very narrow region in the plasma core ($\rho<0.2$) during the NBI phase and the profile is flattened during the LHW pulse. It is understood that the result from AXUV measurement can fully support the result from EUV spectroscopy.

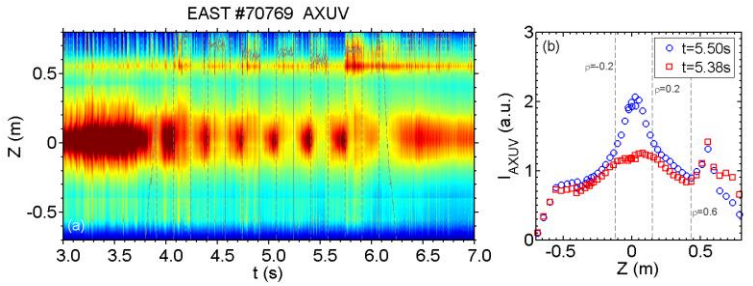

Fig.8 (a)Time evolutions of radiation profile and (b) radiation profiles at two timeslices of t=5.50s (with LHW) and t=5.38s (without LHW) in shot #70769. The injection of LHW is indicated in (a) with gray dashed lines. The vertical locations of $\rho=\pm0.2$ and 0.6 are indicated with vertical dashed lines in (b).

A series of experiments are completed by changing the LHW injection power in the NBI H-mode discharge. Then, the tungsten concentration is analyzed. The result is plotted in Fig. 9 as a function of power ratio of P_{LHW} to P_{NBI}. As a result, it is found that the tungsten concentration starts to decrease at P_{LHW}/P_{NBI}~0.8 and can be sufficiently reduced at P_{LHW}/P_{NBI}~0.9. In this power ratio the tungsten concentration in the plasma core becomes entirely low, e.g. $C_W \sim 5\times10^{-6}$.

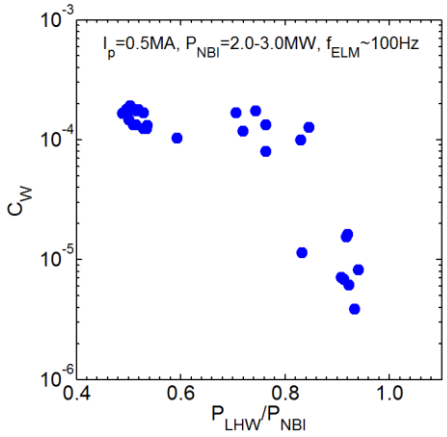

Fig. 9. Tungsten concentration, C_W, as a function of power ratio of P_{LHW} to P_{NBI} in NBI H-mode discharges at $2.0\leq P_{NBI}\leq3.0$MW.

5. DISCUSSIONS

It has been observed in EAST that the tungsten source is increased through enhanced sputtering by energetic ions from big ELMs and NBI beams and carbon ions from lower divertor plates. In addition, the width of scrape-off layer (SOL), λ_q, in NBI H-mode discharges is about half of that in LHW H-mode discharges [25]. It can enhance the tungsten influx entering the plasma in the NBI H-mode discharge. Since the ELM amplitude increases during the LHW phase and energetic particles are created at plasma edge in LHW discharges, the tungsten source is also increased with LHW heating. However, the tungsten accumulation is considerably supressed during the LHW phase in NBI discharges. In particular, the tungsten concentration is much reduced in the region at $\rho\leq0.6$, whereas the tungsten source increases during the LHW phase. Therefore, it is clear that the LHW can change the tungsten transport in both edge and core plasmas.

Tungsten accumulation has been observed during the H-mode phase with big ELMs in high I_p NBI discharges of ASDEX-U [26] and during NBI heating phase in hybrid scenario discharges of JET [27]. In these reports, it is pointed out that an inward neoclassical convection appeared in the central region ($\rho<0.2$) is a main cause of the tungsten accumulation. Recently, it is reported that poloidal asymmetry of high-Z impurities arising from the centrifugal force caused by the strong toroidal rotation in NBI H-mode discharges may enhance the inward flux of high-Z impurities. It may be a main cause of the tungsten accumulation [28]. During the LHW phase in EAST, however, the plasma rotation does not change so much compared with the NBI discharge. On the other hand, the control of the tungsten accumulation is observed in on-axis ECRH discharges of ASDEX-U

[29, 8]. During the LHW phase in EAST the central electron temperature increases from 2.7keV to 3.4keV. Then, the change in the tungsten transport in core plasmas seems to be similar to the ASDEX-U result. When the LHW is applied to the NBI H-mode discharge, the period of sawtooth oscillation is reduced from 30-50ms to 10ms. It may also play an important role in the core tungsten suppression. In EAST it is found that a stochastic layer can be formed in edge magnetic field region with helical currents induced by the LHW [30, 31]. This effect may also enhance the edge impurity screening, in particular, for heavier impurity ions.

6. SUMMARY

Control of the tungsten accumulation is one of crucial subjects to sustain steady-state high performance H-mode in high power NBI discharges. In EAST the plasma performance has been always degraded in NBI H-mode discharges by accompanying with the tungsten accumulation. The tungsten concentration is analyzed against the H-mode performance in NBI discharges. A clear threshold on the tungsten concentration to cause the H-L back transition and plasma disruption is found to range in $6.0\times10^{-5}\leq C_W\leq3.0\times10^{-4}$, not depending on the total heating power. In this work, a beneficial role of the LHW is observed for the first time in EAST for the tungsten accumulation suppression. It is found through the present study that the tungsten accumulation can be controlled by applying the LHW to the NBI H-mode discharge. In EAST, the LHW has an obvious effect on the tungsten suppression when the power ratio of P_{LHW}/P_{NBI} is larger than 0.8. The tungsten concentration is sufficiently reduced at P_{LHW}/P_{NBI}~0.9. The present result demonstrates a possible way toward the steady-state H-mode NBI operation.

ACKNOWLEDGEMENTS

This work was supported by the National Natural Science Foundation of China (Grant Nos. 11575244, 11575247, 11775269), the National Magnetic Confinement Fusion Science Program of China (Grant Nos.2014GB124006, 2015GB101000) and National Key Research and Development Program of China (No. 2017YFE0301300).

REFERENCES

[1] Philipps V., Tungsten as material for plasma-facing components in fusion devices, J. Nucl. Mater. 415(2011) S2-S9
[2] Wan Y., Li J., Liu Y., et al., Overview of the present progress and activities on the CFETR, Nucl. Fusion 57(2017) 102009
[3] Neu R., Balden M., Bobkov V., et al., Plasma wall interaction and its implication in an all tungsten divertor tokamak, Plasma Phys. Control. Fusion 49 (2007) B59.
[4] Bucalossi J., Missirlian M., Moreau P., et al., The WEST project: Testing ITER divertor high heat flux component technology in a steady state tokamak environment, Fusion Eng. Des. 89(2014) 907-912.
[5] Matthews G. F., Beurskens M., Brezinsek S., et al., JET ITER-like wall-overview and experimental programme, Phys. Scr. T145 (2011) 014001.
[6] Yao D., Luo G., Du S., et al., Overview of the EAST in-vessel components upgrade, Fusion Eng. Des. 98-99 (2015) 1692.
[7] Zhang L., et al., "Tungsten control in long pulse H-mode discharges on EAST", TO4.00010, 59th APS-DPP, Wisconsin, US, 2017
[8] Angioni C., Sertoli M., Bilato R., et al., A comparison of the impact of central ECRH and central ICRH on the tungsten behavior in ASDEX Upgrade H-mode plasmas, Nucl. Fusion **57** (2017) 056015.
[9] Lerche E., Goniche M., Jacquet P., et al., Optimization of ICRH for core impurity control in JET-ILW, Nucl. Fusion **56** (2016) 036022.
[10] Goniche M., Dumont R J., Bobkov V., Ion cyclotron resonance heating for tungsten control in various JET H-mode scenarios, Plasma Phys. Control. Fusion 59 (2017) 055001
[11] Hu C. D., Xie Y. H., Xie Y. L., et al., Overview of development status for EAST-NBI system, Plasma Sci. Technol. 17 (2015) 817
[12] Xu H. D., Wang X. J., Liu F. K., et al., Development and preliminary commissioning results of a long pulse 140GHz ECRH system on EAST Tokamak, Plasma Sci. Technol. 18 (2016) 442.
[13] Liu F. K., Ding B. J., Liu L., et al., First results of LHCD experiments with 4.6 GHz system toward steady-state plasma in EAST, Nucl. Fusion 55 (2015) 123022
[14] Zhang L., Morita S., Xu Z., et al., A fast-time-response extreme ultraviolet spectrometer for measurement of impurity line emissions in the Experimental Advanced Superconducting Tokamak, Rev. Sci. Instrum. 86 (2015) 123509.

[15] Zhang L., Morita S., Wu Z. W, et al., A space-resolved extreme ultraviolet spectrometer for radial profile measurement of tungsten ions in the Experimental Advanced Superconducting Tokamak, submitted to Nuclear Inst. and Methods in Physics Research, A
[16] Morita S., Dong C. F., Kato D., et al., Quantitative analysis on tungsten spectra of W^{6+} to W^{45+} ions, Journal of Physics: Conference series.
[17]Zang Q., Zhao J. Y., Yang L., et al., Development of a Thomson scattering diagnostic system on EAST, Plasma Sci. Technol. 12 (2010) 145.
[18] Zhao H. L., Zhou T. F., et al., Upgrade of the ECE diagnostic on EAST, Rev. Sci. Instrum. 89(2018)10H111
[19] Liu H. Q., Jie Y. X, Ding W. X., et al., Internal magnetic field measurements by laser-based POlarimeter-INTerferometer (POINT) system on EAST, JINST 11(2016) C01049.
[20] Zhang S. B., Gao X., Ling B. L., et al., Density profile and fluctuation measurements by microwave reflectometry on EAST, Plasma Sci. Technol. 16 (2014) 311.
[21] Mao H., Ding F., Luo G. N., et al., A multichannel visible spectroscopy system for the ITER-like W divertor on EAST, Rev. Sci. Instrum. 88(2017)043502
[22] Duan Y. M., Hu L. Q., Mao S. T, et al., Measurement of radiated power loss on EAST, Plasma Sci. Technol. **13** (2011) 546.
[23] Zhang L., Morita S., Xu Z., et al., Suppression of tungsten accumulation during ELMy H-mode by lower hybrid wave heating in the EAST tokamak, Nucl. Mater. Energy 12 (2017) 774-778.
[XuW 2018FED][24] Xu W., Sun Z., Hu J. S., et al., Real-time suppression of tungsten impurity influx using lithium powder injection in EAST, Fusion Eng. Des. (accepted)
[25] Wang L., Makowski M. A., Guo H. Y., et al., Effect of heating scheme on SOL width in DIII-D and EAST, Nucl. Mater. Energy 12 (2017) 221-226
[26]Neu R., Dux R., Geier A., et al., New results from the tungsten programme at ASDEX Upgrade, J. Nucl. Mater **313** (2003) 116.
[27] Angioni C., Mantica P., Pütterich T., et al., Tungsten transport in JET H-mode plasmas in hybrid scenario, experimental observations and modelling, Nucl. Fusion **54** (2014) 083028.
[28][casson2015]Casson F., Angioni C., Belli E A., Theoretical description of heavy impurity transport and its application to the modelling of tungsten in JET and ASDEX upgrade, Plasma Phys. Control. Fusion 57 (2015) 014031
[29]Pütterich T., Dux R., Neu R., et al., Observations on the W-transport in the core plasma of JET and ASDEX Upgrade, Plasma Phys. Control. Fusion 55(2013) 124036
[30]Liang Y., Gong X., Gan K., et al., Magnetic topology changes induced by lower hybrid waves and their profound effect on Edge-Localized Modes in the EAST Tokamak, Phys. Rev. Lett. 110 (2013) 235002.
[31] Li J., Guo H., Wan B., et al. , A long-pulse high-confinement plasma regime in the Experimental Advanced Superconducting Tokamak, Nature Phys 9 (2013) 817.